Evaluation of Spatial and Temporal Root Water Uptake Patterns of a Flood-Irrigated Pecan Tree Using the HYDRUS (2D/3D) Model

Sanjit K. Deb[1]; Manoj K. Shukla[2]; Jiří Šimůnek[3]; and John G. Mexal[4]

Abstract: Quantitative information about the spatial and temporal patterns of compensatory root water uptake (RWU) in flood-irrigated pecan orchard is limited. We evaluated spatio-temporal compensated and uncompensated RWU patterns of mature pecan tree in a silty clay loam orchard using the HYDRUS (2D/3D) model. HYDRUS (2D/3D) simulations, which agreed well with measured water contents and temperatures at different soil depths and horizontal distances from the tree trunk, suggested that while both compensated and uncompensated RWU varied with soil depth they did not do so laterally because of similar spatial vertical distributions of root length density (RLD) for the under-canopy and the tree canopy dripline locations. Considering compensated RWU resulted in an increase in actual transpiration by 8%, and a decrease in evaporation and drainage by 5% and 50%, respectively, during a growing season. Simulated transpiration and relative transpiration (a ratio between actual and potential transpiration) values were correlated with measured transpiration and plant-based water stress indicators (stem and leaf water potentials), respectively. Overall, our results of the spatio-temporal compensatory RWU provide support to use HYDRUS (2D/3D) as a tool for managing efficient water use of pecan. **DOI: 10.1061/(ASCE)IR.1943-4774.0000611.**

CE Database subject headings: Silts; Clays; Floods; Irrigation; Evaporation; Trees.

Author keywords: *Carya illinoinensis*; Silty clay loam soil; Root water uptake; Compensated uptake; Flood irrigation; Transpiration; HYDRUS (2D/3D) model.

Introduction

New Mexico is a leading producer of pecans (*Carya illinoinensis*). Pecan trees require large quantities of water during the growing season, and most orchards in the region use flood irrigation to optimize consumptive water use and production of mature pecans. The total amount of water applied using flood irrigation to mature pecans grown at soils with different textures on the Rio Grande floodplain in the Mesilla Valley was reported to range between 1039 and 1977 mm per season (Deb et al. 2012a, 2013). Water availability is considered a major constraint to pecan productivity. With the increased emphasis on water conservation in conflict with the necessity of water availability for pecan production, much effort has been expended over the years on evaluating the amount of water required by a flood-irrigated mature pecan orchard (e.g., Miyamoto 1983; Sammis et al. 2004; Wang et al. 2007). The efficient use of water in flood-irrigated mature pecan orchards and a better understanding of the soil-plant-atmosphere water relations have been repeatedly addressed in recent years (Deb et al. 2011a, 2012b, 2013).

Actual evapotranspiration (ET_a), i.e., actual evaporation (E_a) from the soil and actual transpiration (T_a) from plants, is affected by root zone soil water dynamics and requires simultaneous knowledge of water flow and actual root water uptake (RWU) in soils. Spatial distribution of actual RWU depends not only on the root distribution but also on temporal functioning of the roots as determined by soil water availability. Therefore, efficient water management in flood-irrigated rooting systems depends on the knowledge of spatial and temporal distributions of RWU, as well as on variations of soil water in the root zone. The understanding of spatial and temporal RWU patterns of a mature pecan orchard is also essential for a variety of agricultural and hydrological perspectives, including irrigation management and predictions of yield under water-scarce conditions and of water fluxes to both the atmosphere and the groundwater. However, there remains a paucity of quantitative information about the spatio-temporal RWU patterns of a flood-irrigated mature pecan orchard.

The functioning of roots, whether they are represented microscopically or macroscopically, has received major attention in RWU modeling. A large number of microscopic and macroscopic approaches to model RWU have been proposed over the years and intensely discussed in the literature (e.g., Molz 1981; Feddes and Raats 2004; Green et al. 2006). The microscopic scale model, or single-root model, studies a convergent radial flow of soil water toward a representative individual root, which is idealized as an infinitely long cylindrical sink of a uniform radius. The dynamics and detailed geometry of the rooting system at this microscopic scale are difficult to measure (Vrugt et al. 2001b). In the macroscopic scale approach or a root-system model, a sink term

[1]Postdoctoral Fellow, Dept. of Plant and Environmental Sciences, New Mexico State Univ., Las Cruces, NM 88003 (corresponding author). E-mail: sanjit@nmsu.edu

[2]Associate Professor, Dept. of Plant and Environmental Sciences, New Mexico State Univ., Las Cruces, NM 88003. E-mail: shuklamk@nmsu.edu

[3]Professor, Dept. of Environmental Sciences, Univ. of California Riverside, Riverside, CA 92521. E-mail: jiri.simunek@ucr.edu

[4]Professor, Dept. of Plant and Environmental Sciences, New Mexico State Univ., Las Cruces, NM 88003. E-mail: jmexal@nmsu.edu

Note. This manuscript was submitted on November 8, 2012; approved on March 4, 2013; published online on July 15, 2013. Discussion period open until January 1, 2014; separate discussions must be submitted for individual papers. This paper is part of the ***Journal of Irrigation and Drainage Engineering***, Vol. 139, No. 8, August 1, 2013. © ASCE, ISSN 0733-9437/2013/8-599-611/$25.00.

representing water extraction by the root system is added to the dynamic water flow equation, e.g., the Richards equation (Richards 1931). The first category of macroscopic models is based on steady-state or steady-rate approximations of the single-root models, in which the water flow toward the root system is simulated first, and the total water uptake by the plant is then taken as the sum of the water uptake from each soil layer. The models consider root resistances and water potentials inside and at the root-soil water interface (e.g., Gardner 1964; Hillel et al. 1976), which are difficult to quantify (Wu et al. 1999; Yadav et al. 2009). In the second category of macroscopic models, root water extraction is calculated from the plant transpiration rate, rooting depth, root spatial distribution, and soil water potential. These models take into account the effects of a soil moisture deficit on root water extraction using some response functions dependent on the soil water potential (e.g., Feddes et al. 1978). The parameters in the second category of models are relatively easy to obtain and are generally available in most vadose zone hydrological models (e.g., van Dam et al. 1997; Fayer 2000; Šimůnek et al. 2008).

A multidimensional RWU approach allows more accurate quantification of spatial variability of the soil water regime and water fluxes, especially for an isolated tree in large monocultures where the process of water uptake is complex (Green and Clothier 1999; Vrugt et al. 2001b). Because of the difficulties encountered in measuring spatial and temporal distributions of RWU rates directly in the field, the influence of plant-root systems on water movement can be better understood using variably saturated water flow simulation models, provided that accurate spatial and temporal RWU distributions, particularly compensatory RWU (Skaggs et al. 2006; Šimůnek and Hopmans 2009), are considered. Compensated water uptake, in which plants may respond to nonuniform water stress in the root zone, is a mechanism by which a reduced water uptake in a water-stressed part of the rhizosphere is balanced by an enhanced uptake from another less water-stressed region of the root zone (Jarvis 1989; Šimůnek and Hopmans 2009). HYDRUS (2D/3D) (Šimůnek et al. 2011) is such a numerical model, which simultaneously solves both two- and three-dimensional water flow in homogeneous or heterogeneous soils and both compensated and uncompensated RWU by plants. The model can be utilized to study the interaction between pecan T_a rates and soil water availability. This may provide further insight into how the interaction between soil and roots determines compensated and uncompensated RWU patterns of a flood-irrigated mature pecan tree.

The spatial and temporal distributions of RWU have been mostly reported for microirrigated rooting systems, particularly in sprinkler- and dripper-irrigated orchards (e.g., Vrugt et al. 2001a, b; Koumanov et al. 2006). However, no information is available on the spatial and temporal RWU pattern in a flood-irrigated pecan orchard. In an earlier study on a sandy loam mature pecan orchard, Deb et al. (2011a) simulated the vertical distribution of uncompensated and compensated RWU at an under-canopy location using the HYDRUS-1D model (Šimůnek et al. 2008). These simulations showed that the soil water stress compensation allocated relatively more transpiration to the deeper, less water-stressed depths of the root zone. However, limited to one-dimension, conclusions drawn from this study have raised further questions regarding the spatial and temporal distribution of compensatory RWU in a flood-irrigated mature pecan. The scarcity of information is equally true for pecan orchards in fields with different soil textures in southern New Mexico, particularly in orchards with clayey soil characterized by a much higher water-holding capacity than the sandy loam orchard reported in Deb et al. (2011a). Therefore, the objective of this study was to evaluate spatial and temporal compensated and uncompensated RWU patterns of a flood-irrigated mature pecan tree in a silty clay loam orchard using HYDRUS (2D/3D).

Materials and Methods

Field Site

Field measurements required for the numerical modeling were made over two seasons (March 2009 to December 2010) in a mature, closed-canopy pecan orchard, located at the New Mexico State University Leyendecker Plant Science Research Center (LPSRC), 14.5 km south of Las Cruces, New Mexico. A detailed description of this orchard can be found in Deb et al. (2012a, b, 2013). The experimental region is semiarid, and the study area is dominated by the Harkey-Glendale soil association. A 1.0-ha orchard consisted of seven rows of 30-year-old "Western Schley" pecan trees in a rectangular pattern (7×8 m) with 29 trees in each row. An experimental plot, 50×15 m, consisting of 18 trees in six rows, was located in the middle of the orchard and separated by raised berms.

A single tree in the experimental plot, instrumented with time domain reflectometry (TDR) and soil temperature sensors, was considered in this study. The CS616 TDR sensors (Campbell Scientific, Inc., Logan, UT) were horizontally installed at soil depths of 5, 10, 20, 40, 60, and 80 cm at different distances of 100 (underneath the canopy), 350 (underneath the tree canopy dripline), and 440 cm (just outside of the tree canopy dripline) away from the trunk of a selected pecan tree to continuously monitor the volumetric soil water content (θ) ($cm^3\ cm^{-3}$). For evaluating water contents below 80 cm, we installed two additional TDR sensors at depths of 120 and 160 cm immediately outside of the tree canopy dripline. Sensor data were recorded every 10 min using a CR10X datalogger connected to an AM16/32B multiplexer (Campbell Scientific, Inc., Logan, UT). All TDR sensors were calibrated in situ against gravimetric water content and bulk density data (Deb et al. 2013). We expected that soil temperatures at different distances of 100, 350, and 440 cm from the trunk of the selected pecan tree would be similar in this closed-canopy experimental plot. Therefore, temperature sensors (TMC6-HD, Onset Computer Corp., Bourne, MA) were installed at soil depths of 5, 10, 20, and 40 cm at a distance of 100 cm away from the tree trunk and connected to HOBO H8 4-channel dataloggers (Onset Computer Corp., Bourne, MA) to record soil temperature every 20 min.

The orchard was flood-irrigated using both surface water and groundwater. Six irrigations were applied to the orchard in both the 2009 and 2010 growing seasons. A flow meter was installed to measure both the flow rate and the volume of irrigation water. During an irrigation event, water was applied uniformly across the width of the orchard until the entire orchard was flooded and the berm at the lower end of the orchard prevented tail water from leaving the experimental area. The irrigation water was ponded on the soil surface of the experimental plot, which caused soil water content at the depths of 0–40 cm to remain at near saturation for ~22–26 h as indicated by TDR sensor responses at these depths (data not shown). Weather data obtained from the LPSRC weather station, which is in close proximity to the experimental site, included hourly rainfall, maximum and minimum daily air temperatures, solar radiation, wind speed and direction, and relative humidity measured 2 m above the ground. The experimental site received 302 and 221 mm of rainfall from the day of the year (DOY) 60 to DOY 365 (March 1 to December 31) in 2009 and 2010, respectively.

J. Irrig. Drain Eng. 2013.139:599-611.

Numerical Simulation

We assumed that the RWU around a pecan tree of this closed-canopy orchard was axisymmetrical. Therefore, the axisymmetrical form of the Richards equation could be used to solve the water flow problem. HYDRUS (2D/3D) was used to simulate water flow, heat transport, and RWU processes in an isotropic variably-saturated flow domain. Details on HYDRUS (2D/3D) can be found in Šimůnek et al. (2011). Neglecting the effects of the air phase on water flow, the axisymmetric Richards equation, describing variably-saturated water flow in the axisymmetric flow domain, is

$$\frac{\partial \theta}{\partial t} = \frac{1}{r}\frac{\partial}{\partial r}\left(rK\frac{\partial \psi}{\partial r}\right) + \frac{\partial}{\partial z}\left(K\frac{\partial \psi}{\partial z}\right) - \frac{\partial K}{\partial z} - S(\psi, r, z) \qquad (1)$$

where t = time (d); r = radial coordinate (cm); z = vertical coordinate (positive upward) (cm); ψ = pressure head (cm); $S(\psi, r, z)$ = RWU as a sink term ($cm^3\ cm^{-3}\ d^{-1}$); and K = unsaturated hydraulic conductivity function ($cm\ d^{-1}$). The soil water retention curve and the unsaturated hydraulic conductivity function were estimated using the van Genuchten-Mualem constitutive relationships (van Genuchten 1980; Mualem 1976)

$$\theta(\psi) = \begin{cases} \theta_r + \frac{\theta_s - \theta_r}{[1+(|\alpha_v \psi|^n)]^m} & \psi < 0 \\ \theta_s & \psi \geq 0 \end{cases} \qquad (2)$$

$$K(\psi) = K_s S_e^l [1 - (1 - S_e^{1/m})^m]^2 \qquad (3)$$

where θ_r and θ_s = residual and saturated soil water contents ($cm^3\ cm^{-3}$), respectively; α_v = reciprocal of the air-entry ψ (cm^{-1}); $m = 1 - 1/n$ $(n > 1)$; n = pore-size distribution index (unitless); S_e = effective saturation (unitless) given by $S_e = (\theta(\psi) - \theta_r)/(\theta_s - \theta_r)$; l = pore-connectivity parameter (unitless); and K_s = saturated hydraulic conductivity ($cm\ d^{-1}$). The effects of temperature on soil hydraulic properties (i.e., the soil water retention curve and soil hydraulic conductivity) were taken into account. In HYDRUS (2D/3D), using the capillary theory, the influence of temperature on ψ is quantitatively predicted from the influence of temperature on surface tension (Philip and de Vries 1957). The temperature dependence of $K(\psi)$ is predicted from the influence of temperature on the viscosity and density of water (Constantz 1982).

Neglecting the effects of water vapor diffusion, the governing equation describing the two-dimensional heat transport (i.e., due to conduction and convection with flowing water) in the axisymmetric domain is described by

$$C_p(\theta)\frac{\partial T}{\partial t} = \frac{1}{r}\frac{\partial}{\partial r}\left[r\lambda(\theta)\frac{\partial T}{\partial r}\right] + \frac{\partial}{\partial z}\left[\lambda(\theta)\frac{\partial T}{\partial z}\right] - C_w\frac{1}{r}\frac{\partial}{\partial r}(rqT) - C_w\frac{\partial qT}{\partial z} - C_w ST \qquad (4)$$

where T = temperature (°C); $\lambda(\theta)$ = apparent thermal conductivity of the soil ($J\ cm^{-1}\ d^{-1}\ °C^{-1}$); C_P and C_W ($\approx$4.2 $J\ cm^{-3}\ °C^{-1}$) = volumetric heat capacities ($J\ cm^{-3}\ °C^{-1}$) of the soil and liquid, respectively (de Vries 1963); q = flux density of liquid water ($cm\ d^{-1}$); and the term C_wST = a sink of energy associated with RWU ($J\ cm^{-3}\ d^{-1}$). The $\lambda(\theta)$ in Eq. (4), expressed as a linear function of the velocity, combines the thermal conductivity of the porous medium (solid plus water) (λ_0) in the absence of flow and the macrodispersivity (de Marsily 1986; Šimůnek and Suarez 1993a). The apparent thermal conductivity $\lambda(\theta)$ is given by (Šimůnek and Suarez 1993b)

$$\lambda_{ij}(\theta) = \beta_T C_w |q| \delta_{ij} + (\beta_L - \beta_T) C_w \frac{q_j q_i}{|q|} + \lambda_0(\theta)\delta_{ij} \qquad (5)$$

where subscripts i and j = space direction indices; δ_{ij} (unitless) = Kronecker delta function ($\delta_{ij} = 1$ if $i = j$ and $\delta_{ij} = 0$ if $i \neq j$); and β_L and β_T = longitudinal and traverse thermal dispersivities (cm), respectively. The thermal conductivity λ_0 ($J\ cm^{-1}\ d^{-1}\ °C^{-1}$) is described by the equation of Chung and Horton (1987)

$$\lambda_0(\theta) = b_1 + b_2\theta + b_3\theta^{0.5} \qquad (6)$$

where b_1, b_2, and b_3 = empirical parameters ($J\ cm^{-1}\ d^{-1}\ °C^{-1}$).

The average electrical conductivity of the soil profile (0–100 cm), determined in the 1:2 soil:water suspension at soil depths of 0–20, 20–40, 40–60, 60–80, and 80–100 cm at the end of the 2009 and 2010 growing seasons, was <0.5 $dS\ m^{-1}$. Therefore, the RWU reduction model of Feddes et al. (1978) without the osmotic stress was considered for $S(\psi, r, z)$ in Eq. (1)

$$S(\psi, r, z) = \alpha(\psi, r, z) \times S_p(r, z) = \alpha(\psi, r, z) \times b(r, z) \times T_p \times L \qquad (7)$$

where the water stress response function $\alpha(\psi, r, z)$ = dimensionless function of ψ $(0 \leq \alpha \leq 1)$ (Feddes et al. 1978); $S_p(r, z)$ = potential water uptake ($cm^3\ cm^{-3}\ d^{-1}$); $b(r, z)$ = normalized water uptake distribution (cm^{-2}); T_p = potential transpiration rate ($cm\ d^{-1}$); and L (cm) = surface length associated with transpiration. For $\alpha(\psi, r, z)$, Feddes et al. (1978) proposed a piece-wise linear reduction function parameterized by four critical values of ψ (i.e., $\psi_4 < \psi_3 < \psi_2 < \psi_1$)

$$\alpha(\psi, r, z) = \begin{cases} (\psi - \psi_4)/(\psi_3 - \psi_4), & \psi_3 > \psi > \psi_4 \\ 1, & \psi_2 \geq \psi \geq \psi_3 \\ (\psi - \psi_1)/(\psi_2 - \psi_1), & \psi_1 > \psi > \psi_2 \\ 0, & \psi \leq \psi_4 \quad \text{or} \quad \psi \geq \psi_1 \end{cases} \qquad (8)$$

Water uptake above ψ_1 (oxygen deficiency point, i.e., wetter than some arbitrary "anaerobiosis point") and below ψ_4 (wilting point) is assumed to be zero. Water uptake is maximal between ψ_2 and ψ_3 (reduction point). Between ψ_1 and ψ_2 and between ψ_3 and ψ_4, a linear variation is assumed. The value of ψ_3 depends on the water demand of the atmosphere, and the true ψ_3 is interpolated from low and high values of ψ_3 and T_p.

The $S(\psi, r, z)$ with compensation in Eq. (7), implemented in HYDRUS (2D/3D), was developed by Šimůnek and Hopmans (2009). Following Jarvis (1989), Šimůnek and Hopmans (2009) introduced a critical value of the water stress index (ω_c). The ω_c represents a threshold value above which RWU, reduced in water-stressed parts of the root zone, is fully compensated by enhanced extraction from other less water-stressed parts. In HYDRUS (2D/3D), depending on the value of ω_c, the $S(\psi, r, z)$ represents either compensated ($0.0 < \omega_c < 1.0$) or uncompensated ($\omega_c = 1.0$) RWU. We refer the reader to Šimůnek and Hopmans (2009) for details. The $b(r, z)$ describes the spatial variation of the $S_p(r, z)$ over the root zone and is obtained by normalizing any arbitrarily measured or prescribed root distribution function. Normalizing the uptake distribution ensures that $b(r, z)$ integrates to unity over the flow domain.

HYDRUS (2D/3D) uses the Galerkin finite element method to solve Eqs. (1) and (4), and details can be found in Šimůnek et al. (2011). Fig. 1 shows the considered radially symmetric transport domain with applied boundary conditions. The transport domain, which is 100 cm deep and 450 cm long in the radial direction, was discretized into finite elements using a grid spacing of 2 cm in the radial and 1 cm in the vertical direction. The transport domain was

J. Irrig. Drain Eng. 2013.139:599-611.

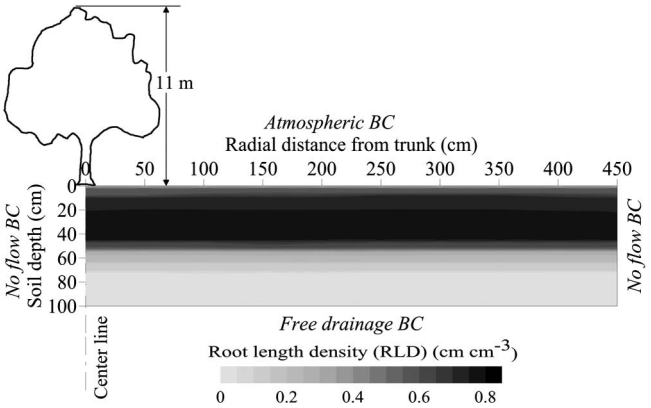

Fig. 1. Axisymmetric flow domain of a flood-irrigated mature pecan tree with considered water flow boundary conditions and spatial root distribution (not drawn to scale)

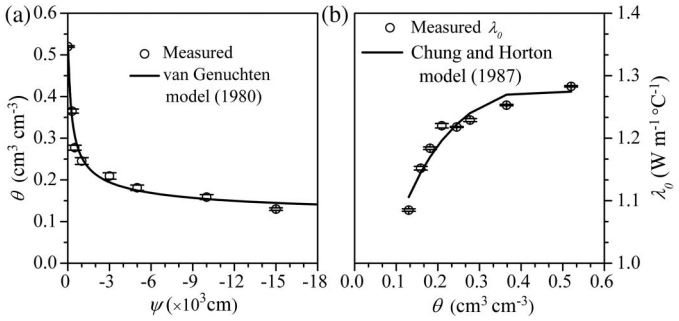

Fig. 2. (a) Water retention curve measured on core samples (θ = volumetric water content and ψ = pressure head), and the van Genuchten (1980) model [Eq. (2)] is fitted to the measured drainage curve using RETC (van Genuchten et al. 1991) ($\theta_r = 0.1$ cm^3 cm^{-3}, $\theta_s = 0.52$ cm^3 cm^{-3}, $\alpha_v = 0.0093$ cm^{-1}, and $n = 1.44$); (b) the thermal conductivity (λ_0) as a function of the volumetric water content (θ), and the nonlinear thermal conductivity equation given by Chung and Horton (1987) [Eq. (6)] is fitted to the measured λ_0-θ relationship (values of regression parameters b_1, b_2, and b_3 are 0.048, −1.76, and 2.37 Wm^{-1}°C^{-1}, respectively)

discretized into 45,000 triangular 2D elements and 22,826 nodes. In general, the soil texture of the orchard was silty clay loam down to a 100-cm soil depth (Deb et al. 2012a, 2013), and thus the soil domain was assumed to be a homogeneous. Observation nodes were located at depths of 5, 10, 20, 40, 60, and 80 cm to coincide with TDR sensor measurements at three radial distances of 100 cm, 400 cm, and 440 cm from the tree trunk.

An atmospheric boundary condition, i.e., the daily potential evaporation (E_p) and transpiration (T_p), and irrigation and rainfall rates were used as the upper water flow boundary condition. For this boundary condition, water evaporates at E_p as long as ψ at the surface remains above a threshold value (ψ_{crit}) of −15,000 cm (Deb et al. 2011a). No flux was allowed through the vertical sides of the transport domain due to symmetry. A free drainage boundary condition was set at the bottom boundary because the water table at this orchard is generally located more than 2.5 m below the soil surface and, therefore, does not influence the root zone soil water dynamics (Deb et al. 2012a). First-type (Dirichlet-type) boundary conditions with specified time-variable temperatures at the soil surface and the bottom were considered for heat transport. Initial conditions were provided by specifying the top and bottom water contents averaged from measured values at 5 and 80 cm and soil temperatures measured at 5 and 40 cm depths and assuming a linear distribution with depth for the 100-cm soil profile.

Measurements and HYDRUS (2D/3D) Parameterization

Soil physical properties down to a 100-cm soil depth at the experimental site were reported in Deb et al. (2012a, 2013). Briefly, the soil texture at the experimental site is silty clay loam, with an average bulk density of 1.5 Mg m^{-3}. The value of K_s ranged from 0.24 to 41 cm d^{-1} within the root zone (0–80 cm soil depth), with an average value of 10.03 cm d^{-1}. Soil water retention was determined using the pressure chamber method at ψ of 0, −300, −500, −1,000, −3,000, −5,000, −10,000, and −15,000 cm H_2O. The initial values of parameters θ_r, θ_s, α_v and n were estimated by fitting the van Genuchten (1980) soil water retention model [Eq. (2)] to the measured drainage curve data using the RETC code (van Genuchten et al. 1991) [Fig. 2(a)]. The initial value of parameter l was assumed to be 0.5 (Mualem 1976).

The core soil samples (three replicates × three tree locations) were collected down to the depth of 40 cm to determine $\lambda_0(\theta)$, the volumetric heat capacity, and the thermal diffusivity using the KD2 Thermal Properties Analyzer (Decagon Devices, Inc., Pullman, WA) at ψ of 0, −300, −500, −1,000, −3,000, −5,000, −10,000, and −15,000 cm H_2O. The nonlinear thermal conductivity equation of Chung and Horton (1987) [Eq. (6)] was fitted to the measured λ_0-θ data, and initial values of regression parameters (b_1, b_2, and b_3) were determined [Fig. 2(b)].

During both growing seasons, 2009 and 2010, soil cores were collected down to a 100-cm soil depth (in 10-cm increments) at distances up to 450 cm away from the trunk of three pecan trees to determine the rooting depth and root length density (RLD) (cm root cm^{-3} soil) distributions for the under-canopy, tree canopy dripline, and just outside of the tree canopy dripline locations. Descriptions of soil core sampling, root extraction procedures, and analysis of RLD can be found in Deb et al. (2013). No roots were observed below 80 cm soil depth (Fig. 1). Similar spatial vertical distributions of RLD for the under-canopy and the tree canopy dripline locations were observed during both growing seasons, 2009 and 2010. The total RLD was higher at shallow depths (0–40 cm) than at the deeper depths (40–80 cm) at all radial distances in this flood-irrigated pecan orchard. For $b(r,z)$ in Eq. (7), a linear root distribution varying between 1.0 (at the soil surface) and 0 (below the depth of 80 cm) was specified.

For $\alpha(\psi,r,z)$, the functional form of RWU parameters given by Feddes et al. (1978) with compensation was used for the HYDRUS (2D/3D) simulations. Deb et al. (2011a) evaluated vertical compensated RWU profiles at different values of ω_c under water-stressed conditions and concluded that the increased compensation from deeper depths was not consistent for lower values of $\omega_c (0.1 < \omega_c < 0.5)$. Therefore, we used a value of $\omega_c = 0.5$ for the soil water stress compensation. Moreover, trial simulations, conducted to evaluate compensated RWU using the critical water stress index (ω_c) below 0.5 ($0.1 < \omega_c < 0.5$), gave similar results or a negligible increase in RWU compared to simulations using ω_c of 0.5. Following the recommendation of Deb et al. (2011a), critical ψ values [Eq. (8)] for the RWU stress function were taken from the HYDRUS (2D/3D) database for a deciduous fruit.

HYDRUS (2D/3D) requires daily potential soil evaporation (E_p) and plant transpiration (T_p) input separately for the atmospheric boundary, i.e., each separately entered into a single atmospheric input. We first estimated daily reference evapotranspiration

J. Irrig. Drain Eng. 2013.139:599-611.

(ET_0) using the FAO-56 Penman-Monteith equation (Allen et al. 1998) based on the weather data. The estimated ET_0 was then multiplied by a crop coefficient (K_c) to estimate pecan evapotranspiration (ET_c). K_c was estimated using the following equations for flood-irrigated mature pecan (Sammis et al. 2004):

$$K_C = -3.866 \times 10^{-12} \times \mathrm{GDD}_i^4 + 1.11 \times 10^{-8} \times \mathrm{GDD}_i^3 - 1.08 \times 10^{-5} \times \mathrm{GDD}_i^2 + 4.31 \times 10^{-3} \times \mathrm{GDD}_i + 3.34 \times 10^{-1} \quad (9)$$

$$\mathrm{GDD}_i = T_{\mathrm{avg}} - T_b \quad (10)$$

where GDD_i = growing degree day value for day i ($T_{\mathrm{avg}} > T_b$, else GDD = 0) (°C day); T_{avg} = average of daily maximum and minimum air temperatures (°C); and T_b = crop-specific base air temperature of 15.5°C for pecan (Sammis et al. 2004; Deb et al. 2012a). Previous studies used Ritchie's formula (Ritchie 1972) (e.g., Vrugt et al. 2001a, b) and/or leaf area index (LAI) (e.g., Droogers 2000) to separate ET_c into E_p and T_p for orchard trees. For partitioning ET_c between E_p and T_p, we calculated E_p using Ritchie's formula (Ritchie 1972) as

$$E_p = ET_c e^{-\kappa \times \mathrm{LAI}} \quad (11)$$

where κ = constant governing the radiation extinction by the canopy as a function of the sun angle, the distribution of plants, and the arrangement of leaves. T_p was then obtained by subtracting E_p from ET_c (Fig. 3). The leaf area index in Eq. (11) was measured on a monthly basis using a LAI-2000 instrument (LI-COR Biosciences, Lincoln, NE) (Deb et al. 2012a). The κ in Eq. (11) was estimated for an ellipsoidal leaf orientation using an equation given by Campbell and Norman (1998). As suggested by Deb et al. (2011a), a spherical leaf angle distribution, which had larger vertical area than horizontal and leaves of all inclinations, was considered in the canopy.

HYDRUS (2D/3D) Calibration and Validation

The HYDRUS (2D/3D) calibration (compensatory RWU option with a ω_c value of 0.5) was performed for a 255-day period from DOY 91 through DOY 365 (April 1 to December 31) 2009. The PEST (parameter estimation) optimization package of Doherty (2004) was used, in which the inverse parameter optimization is achieved using the Gauss-Marquardt-Levenberg method. PEST is a model-independent nonlinear parameter estimator, characterized by an ability to interface with any model through that model's input and output files, thus requiring no alterations to the HYDRUS (2D/3D) model. The calibration process was initiated using measured water flow and heat transport parameters. At the beginning of the model calibration process, we adjusted model parameters in a sequential manner, beginning with water flow parameters and ending with heat transport parameters. Note that we used combined water flow, heat transport, and compensatory RWU processes during the parameter optimization. Selected water flow parameters [i.e., θ_r, θ_s, α_v, n, l, and K_s in Eqs. (2) and (3)] and heat transport parameters [i.e., volume fraction of solid phase, volumetric heat capacities of the solid phase and organic matter, and coefficients b_1, b_2 and b_3 in Eq. (6)] were optimized using measured water content and soil temperature data at measurement soil depths at different radial distances from the tree trunk. Finally, we simultaneously optimized both water flow and heat transport parameters (Table 1). As suggested by Deb et al. (2011a), the ranges of the a priori parameter distribution were derived based on the fits of measured soil water retention data and directly measured λ_0.

The HYDRUS (2D/3D) was validated (compensatory RWU with a ω_c value of 0.5) using the measured and optimized water flow and heat transport parameters for a 306-day period from DOY 60 through DOY 365 (March 1 to December 31) 2010. Once validated, we also used the validated HYDRUS (2D/3D) model to evaluate the spatial and temporal pattern of uncompensated RWU (RWU option with a value of $\omega_c = 1.0$) for the same period. During the HYDRUS (2D/3D) calibration and validation, model predictions of daily average water contents at depths of 5, 10, 20, 40, 60, and 80 cm and soil temperatures at depths of 5, 10, 20, and 40 cm were statistically compared to measured values using the root mean square error (RMSE), the mean bias error (ME) (Shen et al. 1998), and an index of agreement (d) (Willmott 1981), which are defined as:

$$\mathrm{RMSE} = \sqrt{\frac{\sum_{i=1}^{N} (P_i - O_i)^2}{N}} \quad (12)$$

$$\mathrm{ME} = \frac{\sum_{i=1}^{N} (P_i - O_i)}{N} \quad (13)$$

$$\mathrm{d} = 1.0 - \frac{\sum_{i=1}^{N} (P_i - O_i)^2}{\sum_{i=1}^{N} (|P_i - O_{\mathrm{avg}}| + |O_i - O_{\mathrm{avg}}|)^2} \quad (14)$$

where N = number of paired measured and simulated values; P_i = ith simulated value; O_i = ith measured value; and O_{avg} = average of measured values. The value of RMSE reflects a magnitude of the mean difference between measured and simulated results. The value of ME indicates a systematic error or bias in the model prediction, i.e., positive and negative values of ME indicate a tendency for an overprediction or underprediction, respectively. The value of d ranges from 0 (i.e., no agreement) to 1 (i.e., a perfect fit between simulated and measured values).

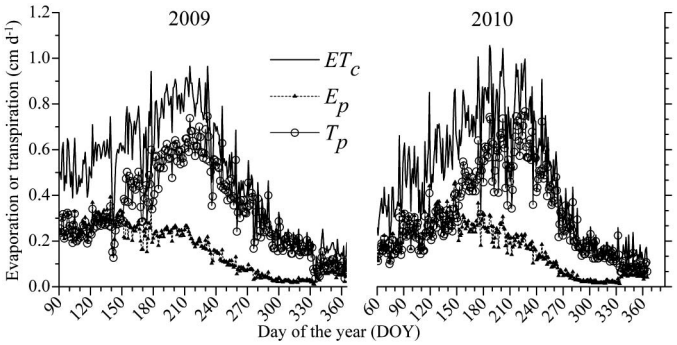

Fig. 3. Potential pecan evapotranspiration (ET_c), soil evaporation (E_p), and transpiration (T_p) during the growing periods from day of the year (DOY) 91 to 365 (April 1 to December 31) of 2009 (the model calibration year) and from DOY 60 to DOY 365 (March 1 to December 31) of 2010 (the model validation year), used as boundary conditions at the soil surface in the HYDRUS (2D/3D) model

Measurements of Transpiration and Plant Water Status

We further evaluated HYDRUS (2D/3D) predictions by comparing simulated actual transpiration (T_a) with measured transpiration (T_{leaf}) and simulated daily soil stress conditions, expressed as the relative transpiration (T_a/T_p), with measured plant-based water

J. Irrig. Drain Eng. 2013.139:599-611.

Table 1. PEST-Optimized Water Flow and Heat Transport Parameters of the HYDRUS (2D/3D) Model during Calibration

HYDRUS (2D/3D) model parameters	Parameter range of a priori parameter distribution	Optimized parameter value
Water flow parameters:		
Saturated soil water content (θ_s, $cm^3\,cm^{-3}$) (van Genuchten 1980)	0.4–0.52	0.48
Residual soil water content (θ_r, $cm^3\,cm^{-3}$) (van Genuchten 1980)	0.09–0.13	0.10
α_v (cm^{-1}) in the soil water retention function (van Genuchten 1980)	0.008–0.09	0.008
n (unitless) in the soil water retention function (van Genuchten 1980)	1.4–2.0	1.44
Tortuosity parameter l (unitless) in the conductivity function (Mualem 1976)	0.5–0.7	0.65
Saturated hydraulic conductivity (K_s, $cm\,d^{-1}$)	0.3–25	10.2
Heat transport parameters:		
Volume fraction of solid phase (θ_n, $cm^3\,cm^{-3}$)[a] (de Vries 1963)	0.48–0.60	0.5
Volumetric heat capacity of the solid phase (C_n, $J\,cm^{-3}\,°C^{-1}$) (de Vries 1963)	1.65–2.20	1.78
Volumetric heat capacity of the organic matter (C_0, $J\,cm^{-3}\,°C^{-1}$)[a] (de Vries 1963)	2.37–3.00	2.51
Coefficient b_1 in the thermal conductivity function ($W\,m^{-1}\,°C^{-1}$) (Chung and Horton 1987)	0.43–0.57	0.47
Coefficient b_2 in the thermal conductivity function ($W\,m^{-1}\,°C^{-1}$) (Chung and Horton 1987)	−0.97 to −1.80	−1.75
Coefficient b_3 in the thermal conductivity function ($W\,m^{-1}\,°C^{-1}$) (Chung and Horton 1987)	2.20–2.64	2.34

[a]Literature value.

stress indicators including midday stem (ψ_{stem}) and leaf (ψ_{leaf}) water potentials.

Transpiration rate (T_{leaf}) (i.e., evaporation from a dry canopy) ($\mu g\,cm^{-2}\,s^{-1}$) was measured from DOY 152 to DOY 273 (June 1 to September 30) 2010 with a steady-state porometer LI-1600 (LI-COR Biosciences, Lincoln, NE). The porometer consists of a cuvette with a broadleaf aperture (2 cm^2), which permits measurements of water loss by transpiration. It measures the flow rate of dry air (<2% relative humidity) necessary to maintain a constant relative humidity (zeroed to ambient relative humidity) inside the cuvette that has been clamped onto a transpiring leaf. Measurements of T_{leaf} during the afternoon (between 1400 h and 1500 h) were taken on five mature, well-exposed leaves for three tree canopy layers, representing lower (at a tree height of 2.5 m from the soil surface), mid- (at 4.6 m), and upper canopy (at 7.6 m). Care was also taken that all leaves were completely dry before any readings were taken. Measured T_{leaf} rates were converted to "$cm\,d^{-1}$", applying the density of evaporated water (1 $g\,cm^{-3}$).

Midday (between 1400 h and 1500 h) ψ_{stem} (for nontranspiring or bagged leaves close to stem) and ψ_{leaf} (for nonbagged leaves) were determined from DOY 152 to DOY 273, 2010 at each of the lower, mid-, and upper canopy layers. Measurements of ψ_{stem} and ψ_{leaf} were made twice a week (every third and sixth day after irrigation) on three selected trees using a pressure chamber (model 1000, PMS Instrument Company, Albany, OR). Details about ψ_{stem} and ψ_{leaf} measurements were described by Deb et al. (2012b).

Results and Discussion

HYDRUS (2D/3D)'s Performance during the Calibration and Validation

Comparisons between measured and simulated daily mean water contents at four depths (5, 10, 20, and 40 cm) at a radial distance of 100 cm from the tree trunk during the calibration period (DOY 91 though DOY 365, 2009) and at different radial distances of 100, 400, and 440 cm during the validation period (DOY 60 though DOY 365, 2010) are shown in Figs. 4(a) and 5, respectively. There was generally a close agreement between measured and simulated water contents for both the calibration and validation periods. Statistics of RMSE, ME, and the index of agreement (d) of simulated and measured θ values, presented in Figs. 4(a) and 5, are comparable with previous modeling studies for flood-irrigated pecan (Deb et al. 2011a, 2012a). For example, RMSE varied between 0.02 and 0.04 $cm^3\,cm^{-3}$, ME between −0.003 and −0.02 $cm^3\,cm^{-3}$, and d between 0.84 and 0.89 during the calibration period [Fig. 4(a)]. Similar discrepancies between simulated and measured θ values were reported by Deb et al. (2011a). During the validation period, RMSE varied between 0.034 and 0.06 $cm^3\,cm^{-3}$, ME between −0.007 and 0.06 $cm^3\,cm^{-3}$, and d between 0.82 and 0.89 for different soil depths and radial distances from the tree trunk (Fig. 5), which represents a good correspondence of the validated model (Deb et al. 2011a, 2012a).

The HYDRUS (2D/3D) predicted both the sharp increase in the water content following irrigation and the gradual decreases during dry-down. However, immediately after an irrigation event, the model predicted higher peak values of θ at depths of 10, 20, and 40 cm, especially during the validation period (Fig. 5), which could be explained by the soil water retention behavior [Fig. 2(a)]. On average, the majority of ME values (Figs. 4(a) and 5) indicated that the model slightly underpredicted θ at most measurement depths. Small differences between simulated and measured θ may be partially explained by measurement errors, which are inevitable under field conditions (Deb et al. 2011a, b, 2012a).

Temporal variations in simulated daily mean soil temperatures for four measurement depths during the calibration and validation periods were consistent with field measurements [Figs. 4(b) and (6)]. For example, RMSE varied between 1.8 and 2.4°C, ME between −0.42 and 1.3°C, and d between 0.93 and 0.98 during the validation period (Fig. 6). Similar discrepancies between simulated and measured soil temperatures were reported in previous modeling studies (Deb et al. 2011a, b), which led us to judge the accuracy of HYDRUS (2D/3D) predictions to be good. Differences between simulated and measured soil temperatures may be partially attributed to the specified initial conditions. Due to the lack of directly measured data below the 40-cm soil depth, initial conditions were simplified, and provided by specifying the top and bottom soil temperatures measured at 5 and 40 cm and assuming a linear distribution with depth. The accuracy of measured and optimized soil heat parameters (Table 1) and the effects of specified surface and bottom heat transport boundary conditions are also possible reasons for the deviations between measured and simulated soil temperatures (Deb et al. 2011a, b).

Spatial and Temporal Root Water Uptake Pattern

Fig. 7 illustrates two-dimensional plots of simulated ψ, θ, and RWU with ($\omega_c = 0.5$) and without ($\omega_c = 1.0$) compensation at DOY 180 and DOY 198 after an irrigation event at 1200 h on DOY 174

J. Irrig. Drain Eng. 2013.139:599-611.

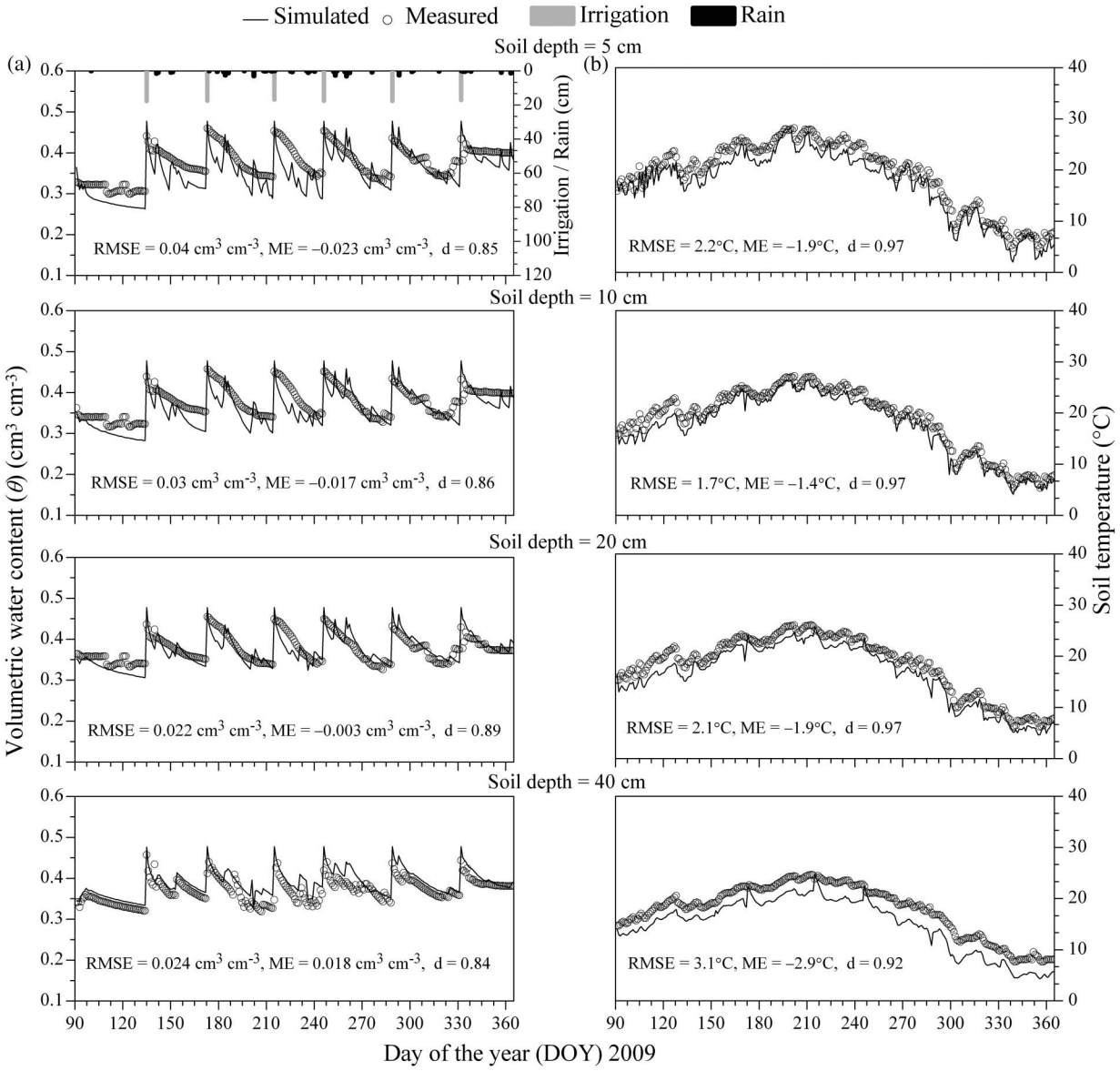

Fig. 4. Comparisons between simulated and measured daily average (a) volumetric water contents and (b) soil temperatures at soil depths of 5, 10, 20, and 40 cm at a distance of 100 cm from the trunk of the pecan tree during the HYDRUS (2D/3D) calibration period from day of the year (DOY) 91 to DOY 365 (April 1 to December 31) 2009. RMSE, ME, and d are the root mean square error, the mean bias error, and the index of agreement [Eqs. (12)–(14)], respectively, between measured and simulated water contents (a) and soil temperatures (b)

during the HYDRUS (2D/3D) validation year 2010. Contour plots for both days were presented at 1430 h because the highest water stress in mature pecans was generally observed in midafternoon (between 1400 and 1500 h) (Deb et al. 2012b). It is clear from contour plots shown in Fig. 7 that both compensated and uncompensated RWU varied with the soil depth but not with distance from the tree trunk under both wet [Fig. 7(a)] and relatively dry soil [Fig. 7(b)] conditions. This is largely attributed to similar vertical distributions of RLD at different radial distances from the tree trunk underneath the canopy and the tree canopy dripline locations (Fig. 1), in accordance with previously reported data during the 2009 growing season (Deb et al. 2013). Furthermore, in this flood-irrigated closed-canopy pecan orchard, Deb et al. (2013) observed that the soil water depletion pattern within the 0–80-cm soil depth varied only depthwise at the under-canopy and outside of the tree canopy dripline locations. Similar observation that the soil water depletion was independent of the horizontal distance in the closed-spaced pecan orchard was also reported by Miyamoto (1983).

The magnitude and pattern of compensated and uncompensated RWU rates were similar 6 days after the irrigation was applied on DOY 174, i.e., at 1430 h on DOY 180, [Fig. 7(a)], and followed the spatially similar vertical distributions of RLD (Fig. 1). The roots extracted water at a higher rate from the upper part of the soil profile (0–40-cm depth) and gradually less from the deeper depths down to 80 cm. The soil profile was slightly drier when the compensated RWU was considered, compared with the uncompensated RWU. For example, θ (or ψ) varied between 0.33 $cm^3\,cm^{-3}$ (−329 cm) and 0.35 $cm^3\,cm^{-3}$ (−234 cm), and between 0.35 $cm^3\,cm^{-3}$ (−252 cm) and 0.38 $cm^3\,cm^{-3}$ (−187 cm) for compensated and uncompensated, respectively [Fig. 7(a)]. However, ψ and θ profiles for the compensated RWU are likely to be more representative since calibration was performed with this option [Fig. 4(a)].

J. Irrig. Drain Eng. 2013.139:599-611.

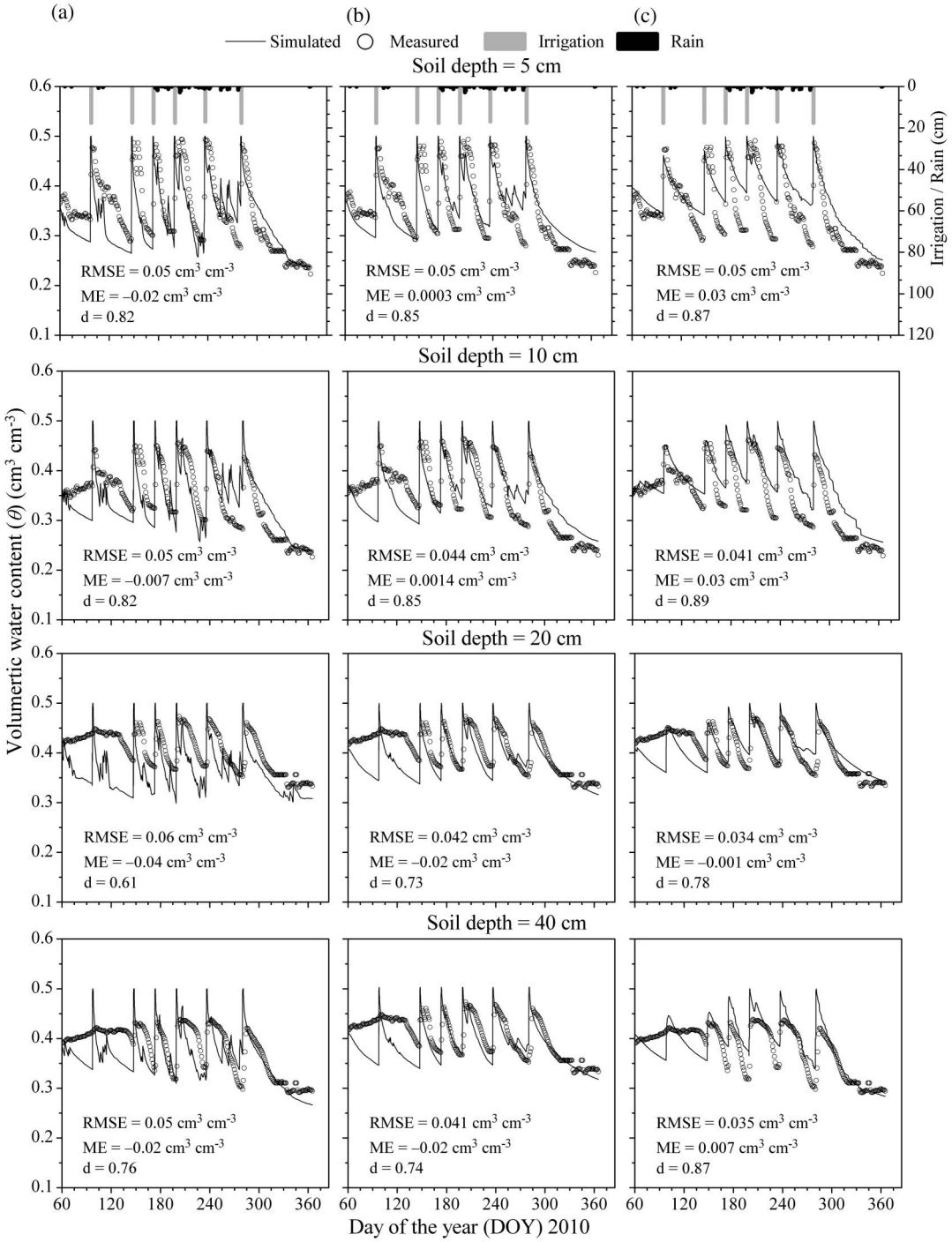

Fig. 5. Comparisons between simulated and measured daily average volumetric water contents at soil depths of 5, 10, 20, and 40 at a distance of (a) 100 cm; (b) 400 cm; (c) 440 cm from the trunk of the pecan tree during the HYDRUS (2D/3D) validation period from day of the year (DOY) 60 to DOY 365 (March 1 to December 31) 2010. RMSE, ME, and d are the root mean square error, the mean bias error, and the index of agreement [Eqs. (12)–(14)], respectively, between measured and simulated water contents

Due to soil drying, both compensated and uncompensated RWU rates generally decreased 25 days after the irrigation on DOY 174 (at 1430 h on DOY 198) [Fig. 7(b)]. RWU increased to a depth of 50 cm as θ values in the upper part of the soil profile (above the depth of 30 and 20 cm for compensated and uncompensated profiles, respectively) decreased ($\theta < 0.16$ cm^3 cm^{-3}), while remaining higher at deeper depths (below the depth of 30 or 20 cm, respectively). Another noteworthy phenomenon is that θ remained relatively high even 25 days after irrigation (Fig. 7), which could be explained by the clayey texture in this orchard. A much lower soil hydraulic conductivity, much higher field capacity, and water-holding capacity resulted in a much slower redistribution of water after irrigation in this silty clay loam soil. Similarly, higher daily average water contents at different soil depths underneath the canopy (radial distances of 100 cm and 400 cm) and outside of the tree canopy dripline (at 440 cm) were observed during the entire growing season (Figs. 4 and 5).

J. Irrig. Drain Eng. 2013.139:599-611.

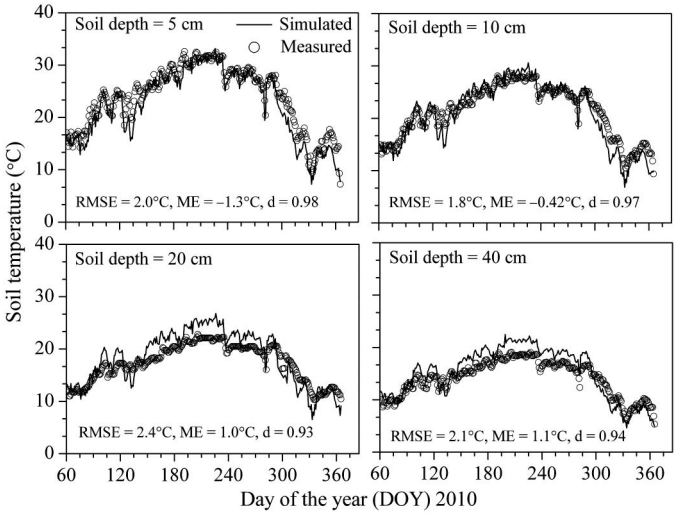

Fig. 6. Comparisons between simulated and measured daily average soil temperatures at soil depths of 5, 10, 20, and 40 at a distance of 100 cm from the trunk of pecan tree during the HYDRUS (2D/3D) validation period from day of the year (DOY) 60 to DOY 365 (March 1 to December 31) 2010. RMSE, ME, and d are the root mean square error, the mean bias error, and the index of agreement [Eqs. (12)–(14)], respectively, between measured and simulated soil temperatures

RWU compensation produced slightly higher RWU rates [Fig. 7(b)]. The compensated RWU pattern differed substantially from the uncompensated on DOY 198 under relatively dry soil conditions. It is possible to distinguish the soil depth where soil water becomes critical for the most efficient RWU by a mature pecan. Even after depletion of water in the top 20 cm, uncompensated RWU was spatially distributed within the upper parts of the root zone (0–50-cm depth). While the upper 30 cm of the soil profile were depleted of water, the depth distribution of compensated RWU was not only governed by the status of soil water but also spatially concentrated in the most densely rooted soil zone or soil layers (30–50 cm).

For evaluating temporal pattern of RWU in the soil profile, Fig. 8 further depicts depth distributions of ψ, θ, and RWU values on different days (i.e., DOY 180, 187, 194, and 198) after the irrigation event on DOY 174 at a radial distance of 100 cm from the tree trunk. Compensated RWU gradually decreased within the upper depths (above 20 cm), and the peak RWU occurred within the depth of 30–50 cm on DOY 198 prior to the subsequent irrigation event on DOY 200 (Fig. 5). In the lower part of the root zone (50–80-cm soil depth) with lower RLD, both compensated and uncompensated RWU rates remained markedly lower and significant variations in θ were not observed between successive irrigation events (Figs. 7 and 8). The spatial occurrence of the highest RLD at soil depths of 30–50 cm would be expected to enhance the ability of pecans to cope with the soil water stress [Fig. 7(b)]. However, had the most densely rooted layer (i.e., the highest RLD) been too shallow (above 20 cm), severe pecan stress due to the water depletion in the upper 20 cm could have caused significant yield loss. Under both wet (nonstressed) and dry (water-stressed) soil conditions, the soil depth (0–50 cm) with higher RLD was the primary RWU uptake layer, and thus water conditions within this layer are more important than the maximum rooting depth of 80 cm (i.e., the effective soil volume for RWU by pecans) to help maintain a certain rate of RWU by pecans. Similar spatial RWU patterns may not have occurred had the pecan root zone had significant variations in RLD both vertically and spatially underneath the canopy and outside of the tree canopy dripline, as well as for nonuniform water applications, such as for microirrigation systems as reported by Koumanov et al. (2006).

Temporal Variation in Actual Transpiration

The simulated actual transpiration of a mature pecan and soil evaporation with and without compensation during the HYDRUS (2D/3D) validation year 2010 are shown in Fig. 9(a). During the period from DOY 60 to DOY 365, T_a was the main contributor to actual evapotranspiration, and the values of compensated and uncompensated T_a varied from 0.06 to 0.80 cm d^{-1} and from 0.04 to 0.70 cm d^{-1}, respectively. Temporal trends of both compensated and uncompensated E_a rates were almost identical, with much smaller values varying from 0.001 to 0.33 cm d^{-1} [Fig. 9(a)]. Soil evaporation occurred only after wetting the surface soil by irrigation or rainfall since the canopy of this closed-canopy orchard helped reduce soil evaporation losses by shading the soil surface and enhancing drying of the soil surface primarily by root water extraction. As shown in Fig. 9(a), a sharp increase in both compensated and uncompensated T_a, particularly from DOY 147 (May 27) to DOY 262 (September 19), was caused by an increase in LAI. Monthly average LAIs varied from 2.0 to 3.4 during this period. The most plausible explanation for sharp drops in simulated T_a immediately after a flood irrigation event is a reduction in RWU as a result of hypoxia under flooded conditions and could be explained by water uptake above critical pressure head ψ_1 in Eq. (8).

Both uncompensated and compensated cumulative values of T_a and bottom water flux are depicted in Fig. 9(b). Cumulative values of compensated T_a remained high and close to potential values, resulting in an 8% increase compared to uncompensated T_a during a 306-day model validation period from DOY 60 to DOY 365, 2010. Deb et al. (2011a) reported that the compensated T_a rates were 15% higher than the uncompensated rates in a flood-irrigated sandy loam mature pecan orchard. It has been reported that the enhanced compensated RWU takes place only after there has been a substantial depletion of water or distribution of water stress across the soil profile (Šimůnek and Hopmans 2009; Deb et al. 2011a). As mentioned earlier, except for a moderate depletion of water within the soil depth above 30 cm, the soil water-holding capacity of the silty clay loam orchard was enough to avoid the severe water stress during the growing season. This explains the relatively lower increase in compensated T_a in our study. As shown in Fig. 9(c), similar temporal trends were observed for the average root zone pressure head (ψ_{RZ}) with and without compensation. Water stress increased in the compensated root zone between successive irrigations, suggesting the enhanced compensatory RWU.

The cumulative bottom drainage was almost 50% less under compensated RWU conditions than without compensation at the end of the 2010 growing season [Fig. 9(b)]. Similarly, cumulative E_a was about 5.1% less during this period for RWU with compensation. Deb et al. (2012a) evaluated deep percolation below a 100-cm vertical soil profile after each irrigation event during the 2009–2010 growing seasons and reported that ~32–36% of the applied water percolated below the root zone in this pecan orchard. From this perspective, simulations with compensatory RWU in our study provided support for using HYDRUS (2D/3D) as a tool to address the water management issue of minimizing water loss via deep percolation.

As shown in Fig. 9(b), the simulated cumulative actual evapotranspiration (ET_a) (per unit area of the axisymmetric domain) (Fig. 1) at the end of the 2010 growing season (DOY 60 through

J. Irrig. Drain Eng. 2013.139:599-611.

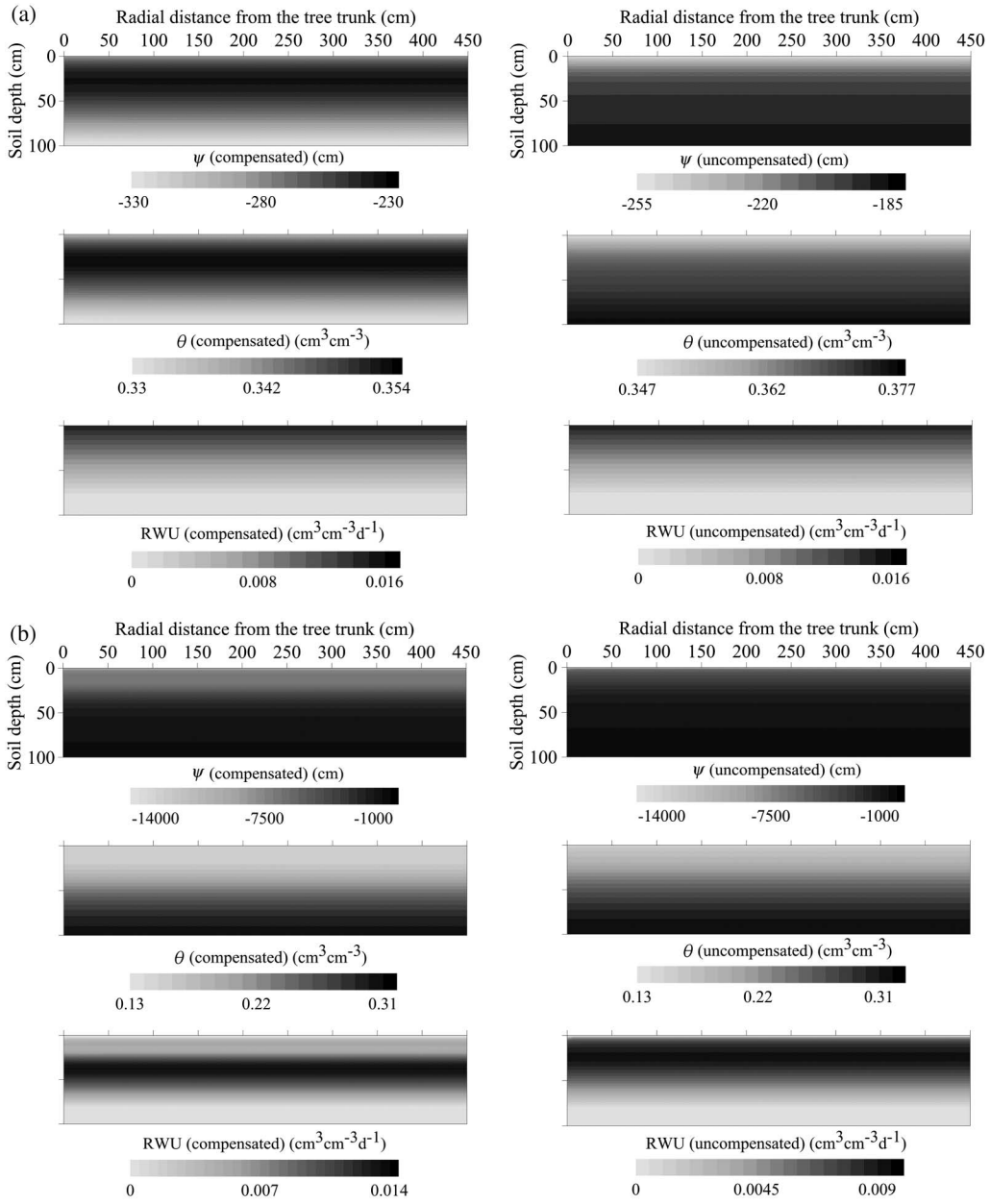

Fig. 7. Spatial distributions of simulated pressure heads (ψ), soil water contents (θ), and root water uptakes (RWU) with ($\omega_c = 0.5$) and without ($\omega_c = 1.0$) compensation after an irrigation event at 1200 h on DOY 174 during the HYDRUS (2D/3D) validation year 2010: (a) at 1430 h on day of year (DOY) 180 (June 29); (b) at 1430 h on DOY 198 (July 17)

DOY 365) was between 124 cm (compensated) and 118 cm (uncompensated). Comparatively, the compensated seasonal ET_a was close to the simulated seasonal potential evapotranspiration (ET_c) of 128 cm. These seasonal ET_a and ET_c predicted by HYDRUS (2D/3D) were reasonable when compared with the seasonal ET_c values reported in previous studies. For example, Miyamoto (1983) estimated the consumptive use of a mature pecan orchard to be 131 cm for the growing season of April through October. Sammis et al. (2004) reported that the total seasonal ET_c of a 30-year-old mature flood-irrigated pecan, measured with the eddy covariance (OPEC) system, ranged from 117 to 126 cm for the growing season of April through November. Samani et al. (2009) estimated the pecan seasonal ET_c using remote sensing, and the maximum seasonal ET_c was 109.5 cm for the growing season of April through October.

We compared daily averages of the simulated compensated and uncompensated T_a rates predicted by HYDRUS (2D/3D) with the measured transpiration (T_{leaf}) for a period from DOY 152 to DOY 273 (June 1 to September 30, 2010) [Fig. 10(a)]. When the measured T_{leaf} was regressed against the simulated compensated and uncompensated T_a during DOY 152 through DOY 273, both compensated ($R^2 = 0.70$) and uncompensated ($R^2 = 0.60$) T_a were significantly ($P \leq 0.05$) correlated with T_{leaf}. However, measured transpiration rates were consistently higher than those predicted by HYDRUS (2D/3D). Relatively higher transpiration rates might relate in part to measurement errors, which were also reported in several studies (e.g., Inoue et al. 1990; Ansley et al. 1994). Air in the porometer cuvette was drier than ambient air, and it was difficult to avoid the porometer leaf chamber warming during afternoon (between 1400 h and 1500 h) readings, particularly at mid- (at 4.6-m

J. Irrig. Drain Eng. 2013.139:599-611.

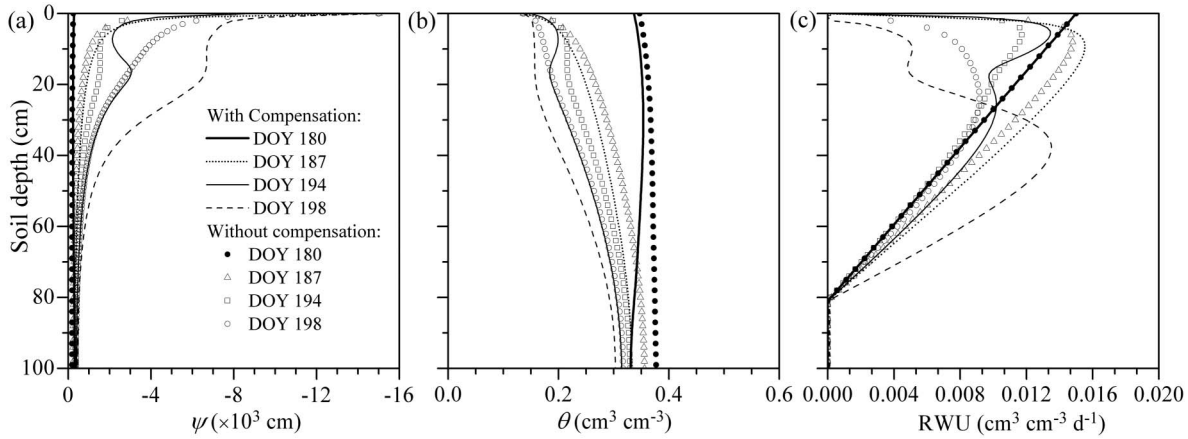

Fig. 8. Depth distributions of simulated (a) pressure heads (ψ); (b) soil water contents (θ); (c) root water uptakes (RWU) with ($\omega_c = 0.5$) and without ($\omega_c = 1.0$) compensation on different days between two successive irrigation events on day of the year (DOY) 174 (June 23) and DOY 200 (July 19) during the HYDRUS (2D/3D) validation year 2010

tree heights) and upper canopy (at 7.6 m) layers where the porometer was continually exposed to ambient conditions. The maximum pecan water stress (i.e., diurnal minimum of ψ_{stem} and ψ_{leaf}) and the higher evaporative demand expressed as the midday atmospheric vapor pressure deficit (VPD) occurred between 1400 h and 1500 h (Deb et al. 2012b), which might also result in a relatively higher T_{leaf}. On the contrary, simulated data [shown in Fig. 10(a)] were mean values of T_a rates that varied during the day.

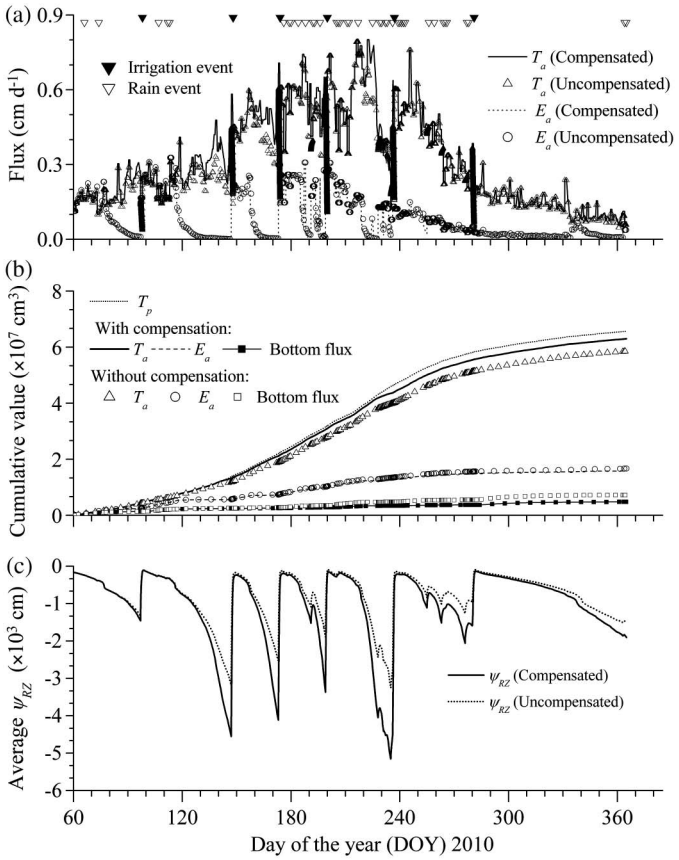

Fig. 9. Temporal variations in (a) actual transpiration (T_a) and evaporation (E_a) rates; (b) cumulative potential transpiration (T_p), cumulative actual transpiration and evaporation, and cumulative bottom water flux (outflow); (c) average root zone pressure heads (ψ_{RZ}) for compensated ($\omega_c = 0.5$) and uncompensated ($\omega_c = 1.0$) root water uptake (RWU) simulations during the HYDRUS (2D/3D) validation period from day of the year (DOY) 60 to DOY 365 (March 1 to December 31) 2010

Comparison of HYDRUS (2D/3D) Simulation with Plant Water Status

The variations in simulated relative transpiration (T_a/T_p) values with and without compensation were consistent with measured plant-based water stress indicators midday ψ_{leaf} and ψ_{stem} [Fig. 10(b)]. Again, the soil water stress compensation could keep the simulated T_a/T_p at a relatively high level to cope with the potential demand of a pecan tree during the growing period. ψ_{stem} was a more stable indicator, as the lower values of ψ_{leaf} compared to ψ_{stem} [Fig. 10(b)] were the result of both T_{leaf} effects on the water potential and desiccation of the leaf following excision during measurement (Deb et al. 2012b). In earlier studies on this orchard, both ψ_{stem} and ψ_{leaf} were significantly correlated with variations in both θ at soil depths down to 40 cm and midday VPD (Deb et al. 2012b). Values of T_a, and in particular, values of compensated T_a, were relatively close to T_p during early periods after irrigation. However, during soil drying, particularly after the depletion of water from the depth of 0–30 cm, the compensated T_a/T_p dropped to a minimum value of 0.42 compared to the uncompensated minimum T_a/T_p of 0.24 during DOY 200 through DOY 238 (July 19 to August 26). This was likely a result of the fact that, during this longer (37d) irrigation interval, the RWU rate may have been high and water available in the root zone did not respond to the T_p demand. This might also be related to the lower soil hydraulic conductivity at the soil-root interface due to the higher clay content of the soil. The decrease in T_a/T_p could be clearly explained by correspondingly sharp decreases in both ψ_{stem} and ψ_{leaf}. For instance, ψ_{stem} varied from −0.64 MPa (nonstressed conditions) to −1.70 MPa (water-stressed conditions) during DOY 200 through DOY 238 [Fig. 10(b)].

Because of much lower magnitudes of soil water depletion within the root zone at this silty clay loam pecan orchard, Deb et al. (2013) recommended that the measured plant water stress indicator ψ_{stem} be used for determining the irrigation date. However, measurements of both ψ_{stem} and ψ_{leaf} using the pressure chamber method are expensive and time consuming, and destructive sampling of stems is required (Deb et al. 2012b). It is also

J. Irrig. Drain Eng. 2013.139:599-611.

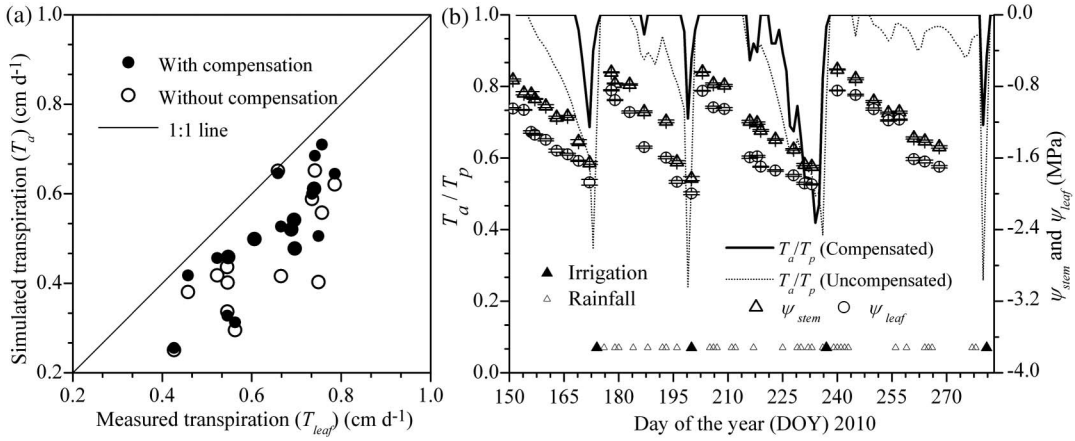

Fig. 10. (a) Simulated compensated ($\omega_c = 0.5$) and uncompensated ($\omega_c = 1.0$) actual transpiration rates (T_a) versus the measured transpiration (T_{leaf}); (b) simulated relative transpiration (ratio between actual and potential (T_p) transpiration), and the midday stem water potential (ψ_{stem}) and the midday leaf water potential (ψ_{leaf}) during the period from day of the year (DOY) 152 to DOY 273 (June 1 to September 30) 2010. T_{leaf}, ψ_{stem}, and ψ_{leaf} values represent mean of the nine measurements, which were made on three trees at three pecan canopy layers, i.e., lower canopy (a tree height of 2.5 m above the soil surface), mid-canopy (at 4.6 m), and upper canopy (at 7.6 m)

difficult to sample multiple trees regularly, especially in a commercial pecan orchard. Alternatively, simulated soil stress conditions predicted by HYDRUS (2D/3D), which are closely related to pecan water stresses (ψ_{stem} and ψ_{leaf}) [Fig. 10(b)], further validate the use of HYDRUS (2D/3D) as a tool for the evaluation of pecan water stress.

Overall, as shown in Fig. 10, as well as in Figs. 4–9 discussed earlier, spatial and temporal distributions of a simulated compensatory RWU of a mature pecan tree suggested that HYDRUS (2D/3D) can be used for managing the efficient water use of flood-irrigated mature pecans while optimizing the pecan production. However, relatively higher plant water stress indicated by ψ_{stem} and ψ_{leaf} for the clayey soils that could hold more water in the root zone between irrigation events lead us to recommend further studies considering the influence of the root resistivity on compensatory RWU by a flood-irrigated mature pecan tree.

Conclusions

HYDRUS (2D/3D) model simulations were found to agree with measured soil water contents and soil temperatures at different soil depths and horizontal distances away from a flood-irrigated mature pecan in a silty clay loam orchard during both calibration (2009) and validation (2010) periods. The RLDs have similar vertical distributions at different distances from the tree: underneath the canopy, tree canopy dripline, and outside of the tree canopy dripline. Similarly to RLD, both compensated and uncompensated RWU patterns of a flood-irrigated pecan varied with soil depth but not with distance from the tree trunk. Both compensated and uncompensated RWU rates were similar during early periods after irrigation. However, the compensated RWU always remained higher in response to the root zone water-stressed conditions, resulting in an increase in compensated actual transpiration (T_a) by 8% and a decrease in actual evaporation (E_a) by 5%, and in bottom drainage by 50% during the 2010 growing season. Spatio-temporal compensatory RWU in this silty clay loam soil, where soil water remained higher throughout the entire root zone between irrigation events, indicated that distribution of roots (the highest RLD within a depth of 30–50 cm) and water content availability within these depths were the most critical factors for maintaining peak RWU rates under dry (water-stressed) soil conditions. Under both wet (non-stressed) and dry soil conditions, the 0–50-cm soil depth with higher RLD was the primary RWU uptake layer, and thus water conditions within this layer were more important than the maximum rooting depth of 80 cm to maintain a certain rate of RWU. Compensated T_a rates predicted by HYDRUS (2D/3D) were correlated with measured transpiration rates under wet and dry soil conditions. The soil water stress compensation could keep the simulated relative transpiration (ratio between T_a and T_p) at a relatively high level to cope with the potential demand of a pecan tree during the growing period. Compensatory T_a/T_p was more consistent with temporal variations in the pecan water stress indicated by both midday stem and leaf water potentials over several irrigation cycles. Overall, our results of the spatio-temporal compensatory RWU simulations provide support for using HYDRUS (2D/3D) as a tool for managing the efficient water use of a flood-irrigated pecan. Similar work with the consideration of the influence of the root resistivity on compensatory RWU patterns is recommended to improve the understanding of model predictions.

Acknowledgments

We thank New Mexico State University Agricultural Experiment Station for support and the Specialty Crop Research Initiative (SCRI), USDA-NIFA for funding this research. We thank Dr. Rolston St. Hilaire, Department of Plant and Environmental Sciences, New Mexico State University, for providing LAI data and the LI-1600 porometer. Our thanks are to Mr. Ramakrishna R. Gopal for his help with PEST, and Dr. Parmodh Sharma and Dr. Pradip Adhikari with field sampling. We also thank Dr. Laurie Abbott, Department of Animal and Range Sciences, New Mexico State University, for allowing us to use plant root washing facilities.

References

Allen, R. G., Pereira, L. S., Raes, D., and Smith, M. (1998). *Crop evapotranspiration: Guidelines for computing crop water requirements*, *FAO Irrigation and Drainage Paper 56*, Food and Agriculture Organization of the United Nations, Rome, Italy.

J. Irrig. Drain Eng. 2013.139:599-611.

Ansley, R. J., Dugas, W. A., Heuer, M. L., and Trevino, B. A. (1994). "Stem flow and porometer measurements of transpiration from honey mesquite (*Prosopis glandulosa*)." *J. Exp. Bot.*, 45(6), 847–856.

Campbell, G. S., and Norman, J. H. (1998). *An introduction to environmental biophysics*, Springer-Verlag, New York.

Chung, S.-O., and Horton, R. (1987). "Soil heat and water flow with a partial surface mulch." *Water Resour. Res.*, 23(12), 2175–2186.

Constantz, J. (1982). "Temperature dependence of unsaturated hydraulic conductivity of two soils." *Soil Sci. Soc. Am. J.*, 46(3), 466–470.

Deb, S. K., Shukla, M. K., and Mexal, J. G. (2011a). "Numerical modeling of water fluxes in the root zone of a mature pecan orchard." *Soil Sci. Soc. Am. J.*, 75(5), 1667–1680.

Deb, S. K., Shukla, M. K., and Mexal, J. G. (2012a). "Simulating deep percolation in flood–irrigated mature orchards with RZWQM2." *Trans. ASABE*, 55(6), 2089–2100.

Deb, S. K., Shukla, M. K., and Mexal, J. G. (2012b). "Estimating midday leaf and stem water potentials of mature pecan trees from soil water content and climatic parameters." *HortScience*, 47(7), 907–916.

Deb, S. K., Shukla, M. K., Sharma, P., and Mexal, J. G. (2011b). "Coupled liquid water, water vapor, and heat transport simulations in an unsaturated zone of a sandy loam field." *Soil Sci.*, 176(8), 387–398.

Deb, S. K., Shukla, M. K., Sharma, P., and Mexal, J. G. (2013). "Soil water depletion in irrigated mature pecans under contrasting soil textures for arid southern New Mexico." *Irrig. Sci.*, 31(1), 69–85.

de Marsily, G. (1986). *Quantitative hydrogeology: Groundwater hydrology for engineers*, Academic Press, Orlando, FL.

de Vries, D. A. (1963). "The thermal properties of soils." Chapter 7, *Physics of plant environment*, W. R. van Wijk, ed., North-Holland Publishing, Amsterdam, Netherlands, 210–235.

Doherty, J. (2004). *PEST: Model-independent parameter estimation, user manual 5th Edition*, Watermark Numerical Computing, Brisbane, Australia.

Droogers, P. (2000). "Estimating actual evapotranspiration using a detailed agro-hydrological model." *J. Hydrol.*, 229(1–2), 50–58.

Fayer, M. J. (2000). *UNSAT-H version 3.0: Unsaturated soil water and heat flow model. Theory, user manual, and examples*, Pacific Northwest National Laboratory (PNNL)-13249, Richland, WA.

Feddes, R. A., Kowalik, P. J., and Zaradny, H. (1978). *Simulation of field water use and crop yield*, Wiley, New York.

Feddes, R. A., and Raats, P. A. C. (2004). "Parameterizing the soil-water-plant root system." Chapter 4, *Unsaturated–zone modelling: Progress, challenges and applications*, R. A. Feddes, G. H. de Rooij, and J. C. van Dam, eds., Wageningen UR Frontis Series, Vol. 6, Kluwer Academic Publishers, Dordrecht, The Netherlands, 95–141.

Gardner, W. R. (1964). "Relation of root distribution to water uptake and availability." *Agron. J.*, 56(1), 41–45.

Green, S., and Clothier, B. (1999). "The root zone dynamics of water uptake by a mature apple tree." *Plant Soil*, 206(1), 61–77.

Green, S. R., Kirkham, M. B., and Clothier, B. E. (2006). "Root uptake and transpiration: From measurements and models to sustainable irrigation." *Agric. Water Manage.*, 86(1–2), 165–176.

Hillel, D., Talpaz, H., and van Keulen, H. (1976). "A macroscopic-scale model of water uptake by a nonuniform root system and of water and salt movement in the soil profile." *Soil Sci.*, 121(4), 242–255.

Inoue, Y., Kimball, B. A., Jackson, R. D., Pinter, P. J. Jr., and Reginato, R. J. (1990). "Remote estimation of leaf transpiration rate and stomatal resistance based on infrared thermometry." *Agric. For. Meterol.*, 51(1), 21–33.

Jarvis, N. J. (1989). "A simple empirical model of root water uptake." *J. Hydrol.*, 107(1–4), 57–72.

Koumanov, K. S., Hopmans, J. W., and Schwankl, L. W. (2006). "Spatial and temporal distribution of root water uptake of an almond tree under microsprinkler irrigation." *Irrig. Sci.*, 24(4), 267–278.

Miyamoto, S. (1983). "Consumptive water use of irrigated pecans." *J. Am. Soc. Hortic. Sci.*, 108(5), 676–681.

Molz, F. J. (1981). "Models of water transport in the soil-plant system: A review." *Water Resour. Res.*, 17(5), 1245–1260.

Mualem, Y. (1976). "A new model for predicting the hydraulic conductivity of unsaturated porous media." *Water Resour. Res.*, 12(3), 513–521.

Philip, J. R., and de Vries, D. A. (1957). "Moisture movement in porous materials under temperature gradients." *Trans. Am. Geophys. Union*, 38(2), 222–232.

Richards, L. A. (1931). "Capillary conduction of liquids through porous media." *Physics*, 1(5), 318–333.

Ritchie, J. T. (1972). "Model for prediction evaporation from a row crop with incomplete cover." *Water Resour. Res.*, 8(5), 1204–1213.

Samani, Z., et al. (2009). "Using remote sensing to evaluate the spatial variability of evapotranspiration and crop coefficient in the lower Rio Grande valley, New Mexico." *Irrig. Sci.*, 28(1), 93–100.

Sammis, T. W., Mexal, J. G., and Miller, D. (2004). "Evapotranspiration of flood-irrigated pecans." *Agric. Water Manage.*, 69(3), 179–190.

Shen, J., Batchelor, W. D., Jones, J. W., Ritchie, J. T., Kanwar, R. S., and Mize, C. W. (1998). "Incorporation of a subsurface tile drainage component into a soybean growth model." *Trans. ASAE*, 41(5), 1305–1313.

Šimůnek, J., and Hopmans, J. W. (2009). "Modeling compensated root water and nutrient uptake." *Ecol. Model.*, 220(4), 505–521.

Šimůnek, J., and Suarez, D. L. (1993a). "Modeling of carbon dioxide transport and production in soil: 1. Model development." *Water Resour. Res.*, 29(2), 487–497.

Šimůnek, J., and Suarez, D. L. (1993b). "UNSATCHEM-2D code for simulating two-dimensional variably saturated water flow, heat transport, carbon dioxide production and transport, and multicomponent solute transport with major ion equilibrium and kinetic chemistry, version 1.1." *Research Report No. 128*, U.S. Salinity Laboratory, Agricultural Research Service, USDA, Riverside, CA.

Šimůnek, J., van Genuchten, M. T., and Šejna, M. (2008). "Development and applications of HYDRUS and STANMOD software packages, and related codes." *Vadose Zone J.*, 7(2), 587–600.

Šimůnek, J., van Genuchten, M. T., and Šejna, M. (2011). *The HYDRUS software package for simulating two- and three-dimensional movement of water, heat, and multiple solutes in variably-saturated media, Technical Manual version 2.0*, PC-Progress, Prague, Czech Republic.

Skaggs, T. H., van Genuchten, M. T., Shouse, P. J., and Poss, J. A. (2006). "Macroscopic approaches to root water uptake as a function of water and salinity stress." *Agric. Water Manage.*, 86(1–2), 140–149.

van Dam, J. C., et al. (1997). "Theory of SWAP, version 2.0, simulation of water flow, solute transport and plant growth in the soil-water-atmosphere-plant environment." *Rep. 71*, Dept. Water Resources, Wageningen Agricultural Univ., *Tech. Doc. 45*, DLO Winand Staring Centre, Wageningen, Netherlands.

van Genuchten, M. T. (1980). "A closed-form equation for predicting the hydraulic conductivity of unsaturated soils." *Soil Sci. Soc. Am. J.*, 44(5), 892–898.

van Genuchten, M. T., Leij, F. J., and Yates, S. R. (1991). "The RETC code for quantifying the hydraulic functions of unsaturated soils, version 1.0." *EPA/600/2–91/065*, U.S. SalinityLaboratory, Riverside, CA.

Vrugt, J. A., Hopmans, J. W., and Šimůnek, J. (2001a). "Calibration of two-dimensional root water uptake model." *Soil Sci. Soc. Am. J.*, 65(4), 1027–1037.

Vrugt, J. A., van Wijk, M. T., Hopmans, J. W., and Šimůnek, J. (2001b). "One-, two-, and three-dimensional root water uptake functions for transient modeling." *Water Resour. Res.*, 37(10), 2457–2470.

Wang, J., Miller, D. R., Sammis, T. W., Gutschick, V. P., Simmons, L. J., and Andales, A. A. (2007). "Energy balance measurements and a simple model for estimating pecan water use efficiency." *Agric. Water Manage.*, 91(1–3), 92–101.

Willmott, C. J. (1981). "On the validation of models." *Phys. Geogr.*, 2(2), 184–194.

Wu, J., Zhang, R., and Gui, S. (1999). "Modeling soil water movement with water uptake by roots." *Plant Soil*, 215(1), 7–17.

Yadav, B. K., Mathur, S., and Siebel, M. A. (2009). "Soil moisture dynamics modeling considering the root compensation mechanism for water uptake by plants." *J. Hydrol. Eng.*, 14(9), 913–922.